Temporal–Spatial Patterns of Relative Humidity and the Urban Dryness Island Effect in Beijing City

PING YANG

China Meteorological Administration Training Center, Beijing, and Department of Atmospheric Science, School of Environmental Studies, China University of Geosciences, Wuhan, and Institute of Urban Meteorology, China Meteorological Administration, Beijing, China

GUOYU REN

Department of Atmospheric Science, School of Environmental Studies, China University of Geosciences, Wuhan, and Laboratory for Climate Studies, National Climate Center, China Meteorological Administration, Beijing, China

WEI HOU

Laboratory for Climate Studies, National Climate Center, China Meteorological Administration, Beijing, China

(Manuscript received 12 October 2016, in final form 12 May 2017)

ABSTRACT

Hourly datasets obtained by automatic weather stations in Beijing, China, are developed and employed to analyze the spatial and temporal characteristics of relative humidity (RH) and urban dryness island intensity (UDII) over built-up areas. A total of 36 stations inside the sixth ring road are considered as urban sites, while six stations in suburban belts surrounding the built-up areas are taken as reference sites. Results show that the RH is obviously smaller in urban areas than in suburban areas, indicating the effect of urbanization on near-surface atmospheric moisture and RH. A further analysis of relations between RH and temperature on varied time scales shows that the variations in RH in the urban areas are not due solely to changes in temperature. The annual and seasonal mean UDII are high in central urban areas, with the strongest UDII values occurring in autumn and the weakest values occurring in spring. The diurnal UDII variations are characterized by a steadily strong UDII stage from 2000 to 0800 LT and a minimum at 1500 or 1600 LT. The rapid shifts of UDII from high (low) to low (high) occur during the periods 0800–1600 LT (1600–2000 LT). The occurrence time of the peaks varies among different seasons: the peaks appear at 0700, 2100, 2000, and 0800 LT for spring, summer, autumn, and winter, respectively. Further analysis shows that large UDII values appear in the evenings and early nights in late summer and early to midautumn and that low UDII values mainly occur in the afternoon hours of spring, winter, and late autumn.

1. Introduction

Because of human activity, land usage and vegetation cover in urban areas have fundamentally changed (Landsberg 1981; Oke 1982; Morris et al. 2001). More and more studies have indicated that energy balances and most climatic elements of urban areas are significantly different from their nearby suburbs (Oke 1988; Ren et al. 2007; Han and Baik 2008; Ren and Zhou 2014; Wang 2014; Yang and Wang 2015). The concept of an urban heat island (UHI), which is one of the most popular topics for scientists in recent years, is a phenomenon in which urban temperature is higher than rural temperature, as has been observed in numerous cities all over the world (Jáuregui 1973; Karl et al. 1988; Liu et al. 2004). To have a better understanding of urban climatology, some scientists have tried to find additional aspects of urban climate instead of being limited to just UHIs (Kratzer 1956; Morris et al. 2001; Dou et al. 2015). Some studies have found that humidity is an important climatic element that is remarkably different in urban areas (Chandler 1967; Ackerman 1971; Hage 1975; Song et al. 2012). The phenomenon whereby the humidity in cities is usually less than that of rural areas has been

Corresponding author: Guoyu Ren, guoyoo@cma.gov

DOI: 10.1175/JAMC-D-16-0338.1

observed for several European cities (Kratzer 1956; Chandler 1967; Lee 1991) and is traditionally referred to as the urban dryness island (UDI) (Hilberg 1978).

Ayoade (1983) proposed that there are six measurements to describe humidity, including absolute humidity, dewpoint temperature, mass mixing ratio, relative humidity, specific humidity, and vapor pressure. Because of its simple mathematical expression and ease of understanding, relative humidity (RH) is one of the most popular measures in the climatological community. Previous studies have demonstrated that RH is a key climatic variable that has an important effect on precipitation, surface water, energy budget, ecological systems, and human physiological comfort levels (Hage 1975). The single characteristics of RH have been indicated by researchers through the long-term power-law correlation of RH records (Padmanabhamurty and Bahl 1982; Li et al. 2016; Kothawale et al. 2016). Numerous studies have demonstrated that the RH in many cities has a decreasing trend that spans several past decades (Zhou 1994; Fortuniak et al. 2006; Song et al. 2012). More comprehensive studies, such as the contrast between city and suburbs, have also been made (Moriwaki et al. 2013; Cuadrat et al. 2015). The fact that urban atmospheres are drier than rural atmospheres has been found in many cities, such as Chicago (Ackerman 1987); London, England (Lee 1991); Belgrade, Serbia (Unkašević et al. 2001); Cairo, Egypt (Robaa 2013); and Zaragoza, Spain (Cuadrat et al. 2015).

In pace with the fast urbanization in China, UDIs have also been found in some big Chinese cities, including Shanghai (Zhou 1994), Beijing (Liu et al. 2009), and Wuwei (Liu et al. 2012). For instance, it was found that the urban–rural humidity differences in Beijing are obvious, and urban environments can decrease the RH at all hours (Liu et al. 2009). In Shanghai, it was concluded that UDIs are always accompanied by an UHI phenomenon (Zhou 1994).

Although RH is a key climatic element, and UDI is an important phenomenon of urban-induced climatological effects, existing research regarding these phenomena is insufficient. In particular, thorough investigations of the UDI structure are lacking because of a lack of high-density observations in urban areas (Zhou 1994; Liu et al. 2009). One of the major issues for most previous studies is an inadequate description of the detailed spatial and temporal patterns of urban RH and UDI in megacities such as Beijing. If the detailed temporal variation is considered, the spatial distribution is often ignored, and vice versa. An important reason for this contradiction is the paucity of relative humidity observations, particularly finite-normal meteorological observations (Yang et al. 2013).

During the twenty-first century, a large number of automatic weather stations (AWSs) have been set up in China, as based on the operational standard issued by the China Meteorological Administration (China Meteorological Administration 2003, 104–125). By 2015, and taking Beijing as an example, a dense AWS network with more than 200 stations has been established (Yang et al. 2011, 2013). About one-half of the stations attached to the network can provide hourly RH data.

In this paper, we investigated the hourly RH data obtained by AWSs in Beijing, and the climatological temporal–spatial features of RH and UDI intensity (UDII) are discussed in detail. In the following sections, station information and basic climatological characteristics of RH are introduced first; then the spatial distribution, seasonal variation, and diurnal cycle of UDII in urban areas are examined; finally, the causation of the UDII variation is discussed briefly before the conclusions are drawn.

2. Study area, data, and analysis methods

Beijing municipality, the capital of China, with 1.6 million km^2 of area, lies to the north of the north China plain and to the south of the Yanshan Mountains. Most parts of the plain have an elevation of 100 m above sea level or less (Fig. 1a). Beijing has a typical continental monsoon climate with four distinct seasons. Spring is dry and windy, autumn is calm, summer is hot and rainy, and winter is dry and cold (Yang et al. 2017).

With rapid urbanization, the population in Beijing city is swiftly increasing. The total number residents in Beijing reached 20 million in 2010, which is double the census result from 1986. Along with the bewildering urban sprawl, express transportation systems have become a necessity in Beijing city, and a multiple–ring road (RR) (including the fourth RR, fifth RR, and sixth RR) system of transportation (as seen in Fig. 1b) has been developed (Wang et al. 2010; Yang et al. 2013).

Following the classification by Yang et al. (2013), Beijing city, with 42 stations (36 urban sites and 6 reference sites) was chosen as the study area in this paper. Thirty-six stations inside the sixth RR were considered as urban region (UR) sites, while those inside the fourth RR (17 stations) were considered as urban center (UC) sites (Fig. 1b). Six reference stations surrounding the urban region were selected via a remote sensing method developed by Ren and Ren (2011). The average elevation of the six reference stations is very similar to those of the urban stations within the different RRs (Yang et al. 2013), and thus the observational records between the reference and urban stations are comparable.

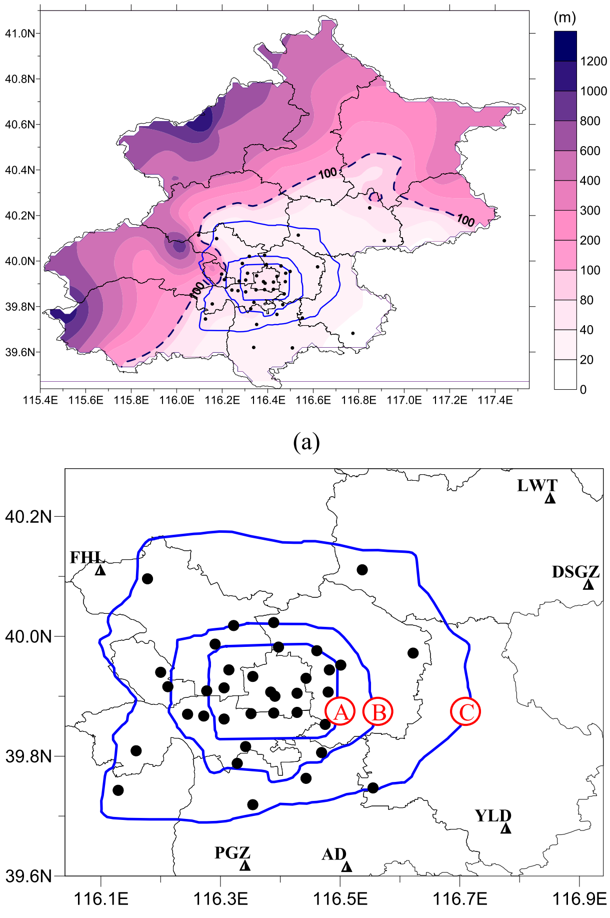

FIG. 1. Distribution of AWSs used in the study. (a) The locations of AWSs used in the whole area over the Beijing municipality. (b) Stations in the Beijing urban region as outlined by the sixth RR (blue solid circles; enclosing lines A–C represent the fourth, fifth, and sixth RR, respectively) and the six rural stations outside the sixth RR. [Station names are Feng Huang Ling (FHL), Yong Le Dian (YLD), Pang Ge Zhuang (PGZ), An Ding (AD), Nan Zhao (NZ), Da Sun Ge Zhuang (DSGZ), and Long Wan Tun (LWT).]

The hourly RH data from the 42 stations in Beijing city during 2007–15 were obtained from the Meteorological Information Center, Beijing Meteorological Bureau. To increase the robustness of our analyses, all hourly RH data have been quality-controlled, and possible erroneous data were detected, evidenced, and adjusted. A few of missing values were replaced by the instantaneous valid values of its nearest five stations, using the spatial interpolation of the inverse distance weighing technique (Lin et al. 2002; Yang et al. 2011, 2013).

In this study, the UDII was estimated by calculating the difference in the RH between urban and rural areas. The rural RH (RHr) is the average RH of the six reference stations, and the urban RH (RHu) is the RH of any urban station, or the averaged RH values of the urban stations inside any specific urban areas. UDII therefore can be defined as

$$\mathrm{UDII} = -(\mathrm{RHu} - \mathrm{RHr}). \tag{1}$$

3. Temporal–spatial distribution of RH

a. Spatial characteristics of RH

The annual mean RH over the study area is shown in Fig. 2. During the 9-yr period, the annual mean RH is 53.2%, with the lowest value (47.1%) appearing in Wu Ke Song (WKS) near the joint belt of the urban center and Hai Dian (HD) district. The highest record (59.8%) is seen in Pang Ge Zhuang (PGZ), which is one of the reference sites in the southwestern Da Xing (DX) district. Relatively lower RH centers can be identified inside the urban center or zones adjacent to the fourth RR. In the east, the mean RH is generally higher than that in the west.

Similar to the annual spatial distribution, stations with remarkably low mean RH values for each season are mostly concentrated in the area inside the fourth RR (Figs. 3a–d), and those with high mean RH values appear in regions farther away from the urban center. Nevertheless, the differences of spatial distribution among different seasons are also obvious. The highest seasonal mean RH over Beijing city takes place in summer. A previous study also found that large RH more easily occurs in the season or area with heavy rainfall (Zhang et al. 2011). Therefore, the highest RH in summer is quite possibly related to the heavy precipitation of Beijing occurring during this season. In contrast, the regional difference in RH is weakest in spring. As seen in Fig. 3a, the site-to-site difference between the maximum and minimum mean RH values during spring does not exceed 10%. The mean RH differences among the sites are consistently larger in summer than those in spring; however, they increase in autumn and winter. The largest site-to-site difference of the seasonal mean RH values, 15.6%, occurs in autumn. Obviously, the large spatial contrasts of the annual mean and seasonal mean RH values mainly result from UDI effects, which lead to a significant decrease in the RH over built-up areas when compared with the surrounding countryside.

b. Temporal characteristics of RH

Figure 4 displays the annual and seasonal mean diurnal cycle of the RH over Beijing city. It is clear that a diurnal variation in the RH is apparent. The annual

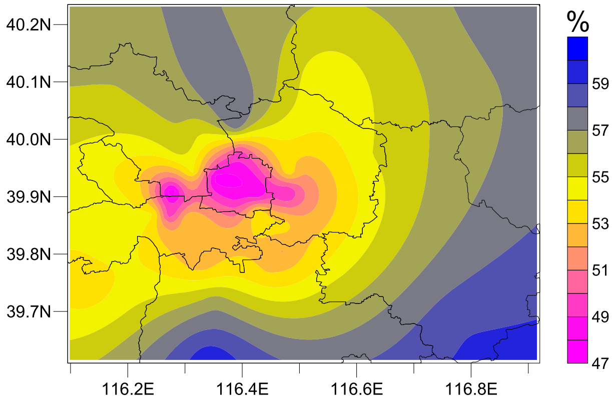

FIG. 2. Spatial distribution of the annual mean values of RH in Beijing city during 2007–15.

mean RH value reaches a minimum of 37.5% at 1500 and a maximum of 67.2% at 0600 during a day cycle (Fig. 4a). A similar diurnal variation was also found by Fortuniak et al. (2006) in Lodz. It is easily seen that the diurnal RH curve is completely opposite to that of the surface air temperature (Yang et al. 2013), with the higher (lower) values of RH corresponding to the lower (higher) surface air temperature in a day.

Figure 4b shows the diurnal RH variations for different seasons. Obviously, similar diurnal variations appear in different seasons in accordance with the diurnal variation throughout the year. The maximum RHs are all in the early morning, and the minimum values occur in the afternoon. However, the differences among the seasons are also evident. The mean RH values in the summer at all hours are higher than those in the other seasons. The diurnal variations of seasonal mean RH in the winter and spring are lower and similar to each other; the distinction between winter and spring is that the hourly mean values in spring are higher than those in winter during the early morning (0200–0700 LT), while the opposite is true for the remaining hours.

To examine detailed seasonal characteristics, comparisons of diurnal features in different seasons are shown in Table 1. It is obvious that the seasonal mean RH value ranges from 42% to 67%, with summer seeing the largest value, autumn the second largest, and winter the smallest. All seasonal mean RH values peak during the early morning, despite the fact that the accurate appearance times are not in full accord. The peak values appear respectively at 0600, 0500, 0600, and 0700 LT from spring to winter. It is obvious that the peak appearance time is the earliest in summer and the latest in winter. This is in accordance with the seasonal surface air temperature variation (Yang et al. 2013), which is probably caused by variations in solar irradiance due to

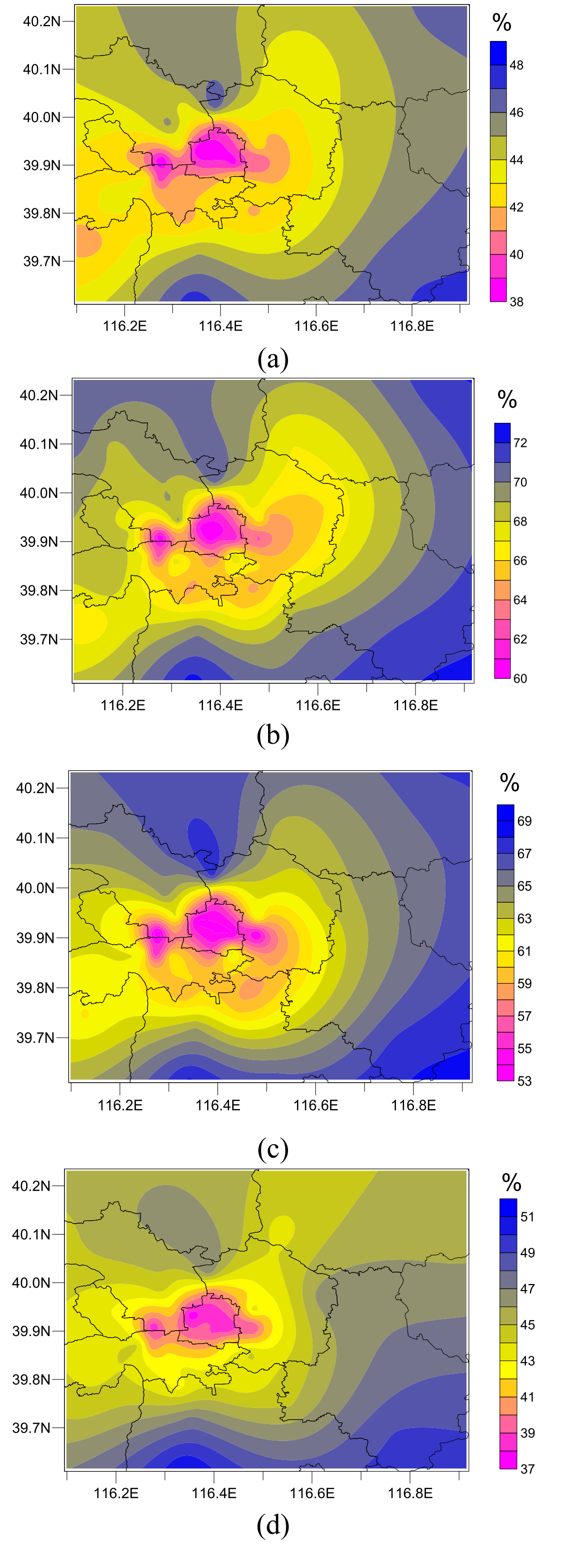

FIG. 3. Spatial distributions of RH in (a) spring, (b) summer, (c) autumn, and (d) winter in Beijing city. during 2007–15.

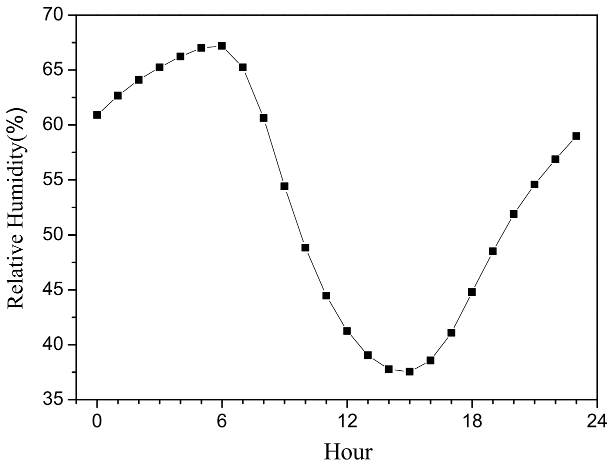

(a)

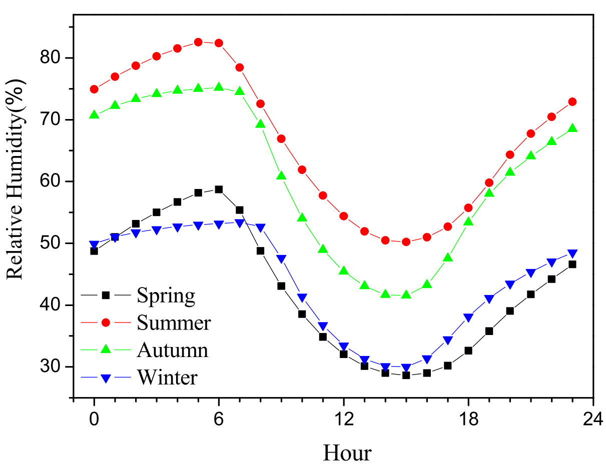

(b)

FIG. 4. Diurnal variations of (a) annual mean value and (b) seasonal mean values of RH in Beijing city during 2007–15.

the varied sunrise time during the different seasons. Different from the peak appearance times, all of the appearance times of the diurnal RH valley are reached at the same time of 1500 LT.

The combined annual and seasonal variation in the monthly mean RH values and the monthly mean RH anomaly values are shown in Fig. 5. The temporal pattern indicates that there is a prominent seasonal variation during the study period. The monthly mean RH value is large in July, August, and September, while it is small in winter and spring months. These seasonal variations differ slightly from year to year. For example, the value of RH in December 2015 is apparently larger than those in other years. To reveal the year-to-year variations, isolines based on the monthly mean RH anomaly values are given in Fig. 5b. The annual variation is easier to be seen in the month–year RH anomaly profile. In January and February, the RH anomaly was positive in 2008, 2011, and 2012. It also appears to have been positive in November and December of 2010, 2013, and 2014. In January of 2013 and November and December of 2015, the RH anomaly value was obviously negative.

Hour–year profiles of the hourly mean RH values and the hourly mean RH anomaly values are shown in Figs. 6a and 6b, respectively. In Fig. 6a, it is noteworthy to point out the marked diurnal variation. During the daytime, the hourly mean RH value maintains smaller values from 1200 to 1600 LT, and changed to larger values during 0400–0700 LT. The decreasing rate in the morning is much larger than the increasing rate in afternoon and early evening, as seen from the denser isolines during 0700 and 1000 LT and the sparser isolines during 1700 and 2000 LT in Fig. 6a.

To examine the year-to-year variation more clearly, the combined annual and diurnal variations of the hourly mean RH anomaly values are shown in Fig. 6b. It is interesting to note that after 2010 the interannual oscillation was more significant. The mean hourly RH anomaly values were positive at all hours in 2011 and 2012 but negative for all of 2013 and 2015 during the daytime. The similar characteristic was not found for the years before 2010. During 2007–10, a relatively obvious seasonal variation occurred from noontime to nighttime. During the period of 1200–1700 LT, the value was the largest in 2007–09 and the smallest in 2010. From 1800 to 2300 LT, smaller values appeared in 2007, 2008, and 2010, but it was larger in 2009. The reason for the shift of the seasonal variation pattern is unknown, and a further investigation into this issue is needed. The temporal–spatial variations in the RH values indicate that the RH levels in urban areas are different from those in rural areas, and variations in the RH on different time scales are complicated.

TABLE 1. Diurnal features of RH among different seasons in Beijing city during 2007–15.

		Spring	Summer	Autumn	Winter
Seasonal mean value (%)		42.5	66.5	60.7	43.8
Daily peak	Value (%)	58.7	82.6	75.2	53.4
	Appearance time	6 h	5 h	6 h	7 h
Daily valley	Value (%)	28.6	50.2	41.6	30.0

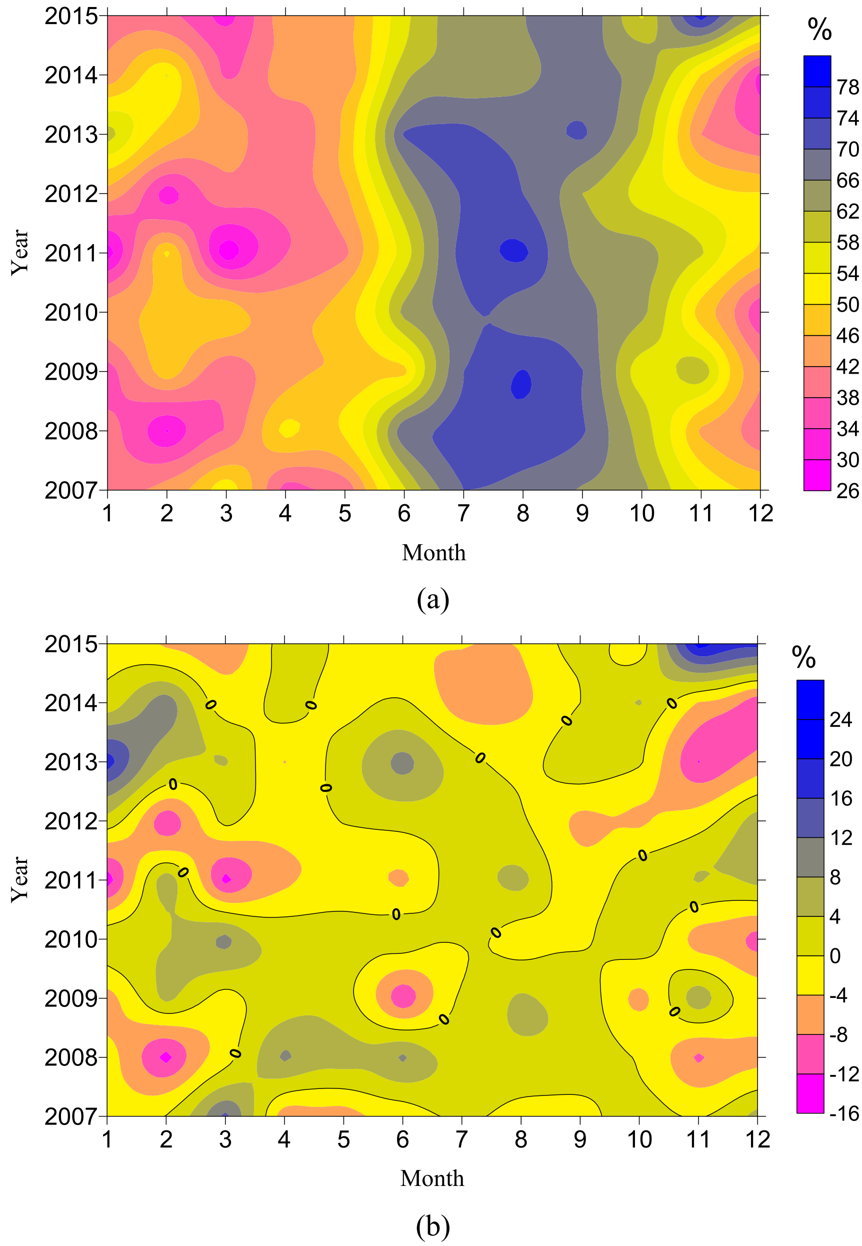

FIG. 5. Month–year plot of (a) mean RH and (b) mean RH anomaly [0% isolines are labeled in (b)].

4. Temporal–spatial pattern of UDII

a. Spatial distribution of UDII

The spatial distribution of the annual mean UDII values over urban areas (corresponding to the built-up areas inside the sixth RR) is shown in Fig. 7. The maximum UDII center (10.5%) appears at WKS (39.9°N, 116.3°E), in the southwestern part of Hai Dian, which coincides with the high center of the RH in Fig. 2. It is also obvious in Fig. 7 that the largest UDII value, with 8% (marked by green lines) or greater, mostly occurs in the UC inside the fourth RR (ranging from 8% to 11%). The only station with a small negative UDII value (−0.09%) is Olympic Green (OG; 40.0°N, 116.4°E), which is to the north of the built-up areas. Although OG is located near the outside of the fourth RR, it is a large park covering 11.35 km^2. Previous investigations have demonstrated that urban parks can reduce the UHI effect because of the abundance of trees and grass (e.g., Yang et al. 2016). The negative UDII value measured

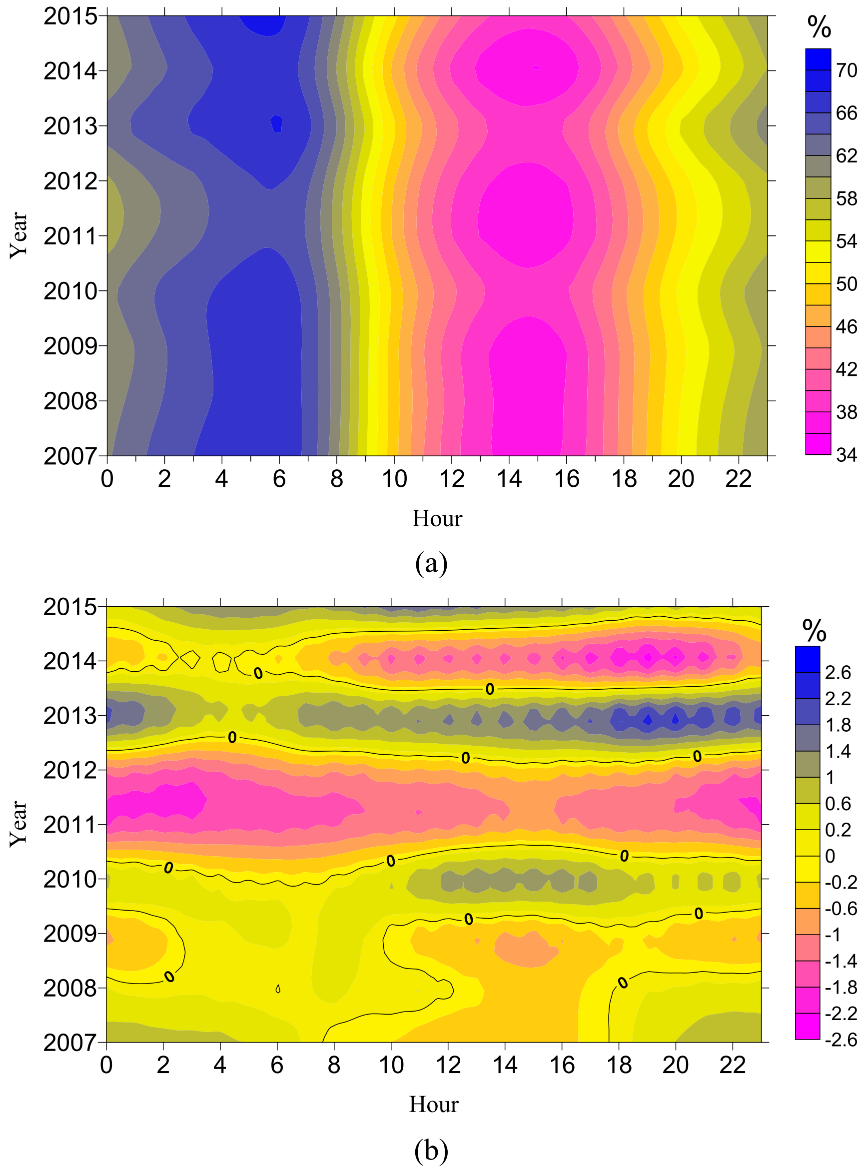

FIG. 6. As in Fig. 5, but for hour vs year.

for OG is related to the reduced UHI effect and more atmospheric moisture near the surface due to the evapotranspiration in the park.

Figure 8 shows the spatial distribution of the seasonal mean UDII values over urban areas in Beijing. It is obvious that the UDII is stronger in autumn and summer than in winter and spring, as indicated by the sizes of the areas surrounded by the green isoline of 8%. Spring registers the weakest UDII during 2007–15. The UDII in spring is so weak that whole areas have records of less than 8%, which cannot be shown in the figure. The seasonal mean UDII is stronger in summer, where the 8% isoline covers an extensive area, and the maximum UDII value in WKS exceeds 11.2%. In autumn, the seasonal mean UDII experiences a considerable increase, where the 8% isoline covers the largest area around the fourth RR among the four seasons, which propagates from the center to east and west along the same latitude. The maximum UDII in WKS reaches 13.8%. The seasonal mean UDII is slightly larger in winter than that in spring, and the area of values exceeding 8% only includes a small extent in the center of the fourth RR.

It was found that the UHII is also the weakest in spring in Beijing city (Yang et al. 2013; Dou et al. 2015) mostly probably because of stronger wind speeds, the

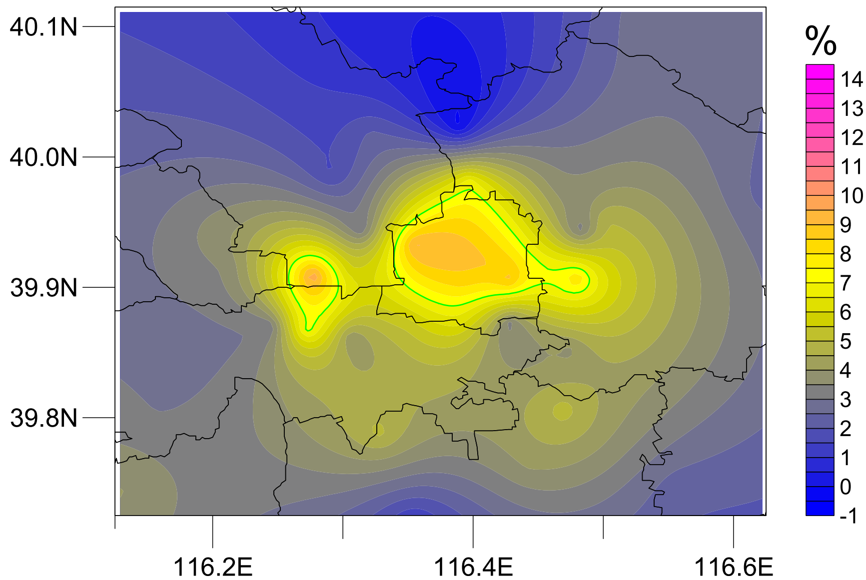

FIG. 7. Spatial distributions of annual mean values of UDII in the urban area over Beijing during 2007–15. The green line represents the 8% isoline of the annual mean UDII.

spatial difference of surface air temperature within the urban areas, and also the temperature difference between urban areas and rural sites. This may be the main reason for the weak UDII in spring. Although the highest UHII is found in winter in many temperate cities including Beijing city, the seasonal mean UDII in winter is not the strongest among four seasons, nor is it the weakest. This is because the RH and UDII are determined by both air temperature and atmospheric moisture. Although the seasonal mean UHII is the strongest in winter, the difference in moisture content and the RH between urban and rural sites is not necessarily larger than that in spring, and the winter mean UDII does not register its lowest value.

b. *Temporal characteristics of UDII*

Figure 9 displays the pentad and hourly mean UDIIs over UR represented by the 36 urban stations and UC represented by the 17 urban stations inside the fourth RR. Similar variations appear in the UC and UR values, but there is an apparent difference between the two domains throughout the year. The difference clearly indicates that the UDI effect over the UC is larger and more significant. The UDII in UR is lower than that in UC at any pentad. Figure 9a also shows that UDIIs in autumn are much higher than those in any other season. This is consistent with the above-mentioned features shown in Fig. 8. The average pentad difference in the UDII between UC and UR is 1.7%, and that in autumn (from the 48th pentad to 66th pentad) is 2.2%, suggesting that the UDI effects are the largest in autumn.

Figure 9b shows the difference of diurnal UDII variations between UC and UR. Similar to Fig. 9a, the difference between the UC and UR stations is evident and the UDII in UC is higher at any time during a day. The daytime (especially 1000–1800 LT) UDII contrast between UC and UR is smaller. The maximum UDII value occurs in the early morning (0700 LT) and the minimum UDII values in the afternoon (1600 LT) for both UC and UR. Therefore, the UDII values of UC exhibit more diurnal variability than those of UR. Figure 9 also shows that the temporal variations of the UDII values of UC and UR are similar except for the fact that the former is obviously larger than the latter. Therefore, in the following analysis, focus is given on to the temporal features of the UR UDII values.

Figure 10 presents the diurnal course of UDIIs in the four seasons. The diurnal variations of the different seasons are similar to the mean hourly UDII values of a year with maxima around the early morning and nighttime and minima in the afternoon (1500 or 1600 LT). However, differences in the diurnal behavior among the different seasons are also obvious. First, although the appearance time of valleys is similar (1500 or 1600 LT), the occurrence of peaks is distinctly different among the different seasons. The respective appearance time of the peaks is 0700, 2100, 2000, and 0800 LT from spring, summer, autumn, and winter (Fig. 10 and Table 2). It is evident that evening time (1900–2100 LT) and early morning (0700–0800 LT) are two periods with larger UDI effects, with the UDII peaks of winter and spring in the morning and those of summer and autumn in the

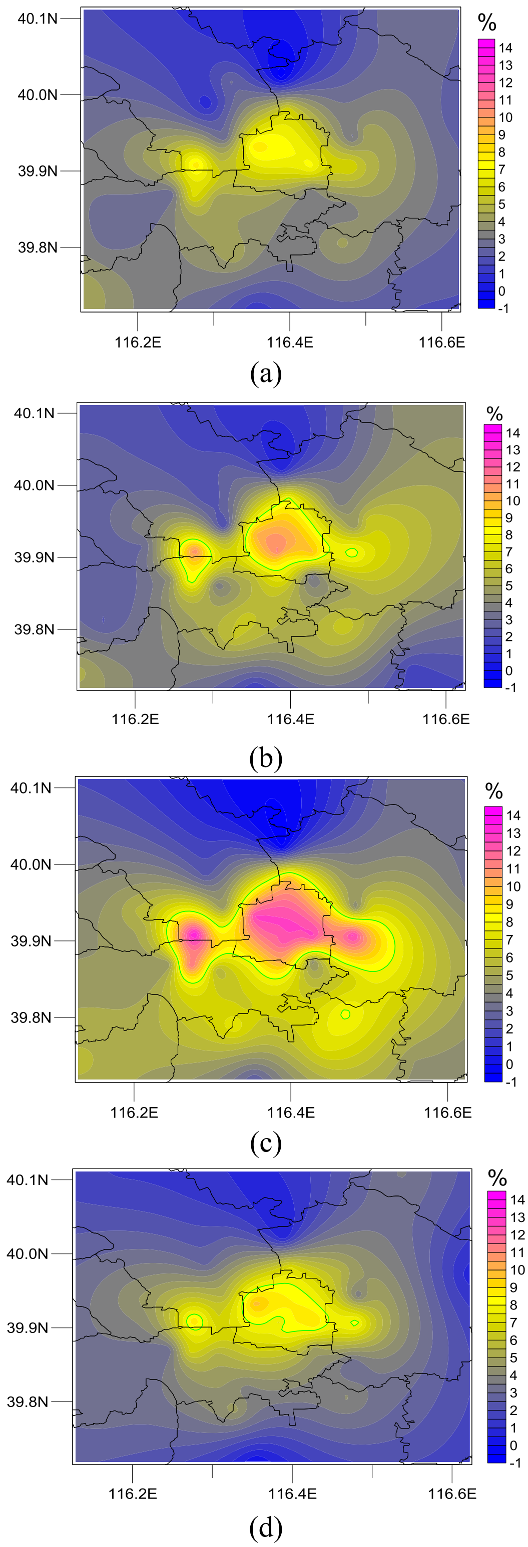

FIG. 8. Spatial distributions of UDII in (a) spring, (b) summer, (c) autumn, and (d) winter in the urban area of Beijing during 2007–15. Green lines represent the 8% isoline of seasonal mean UDII.

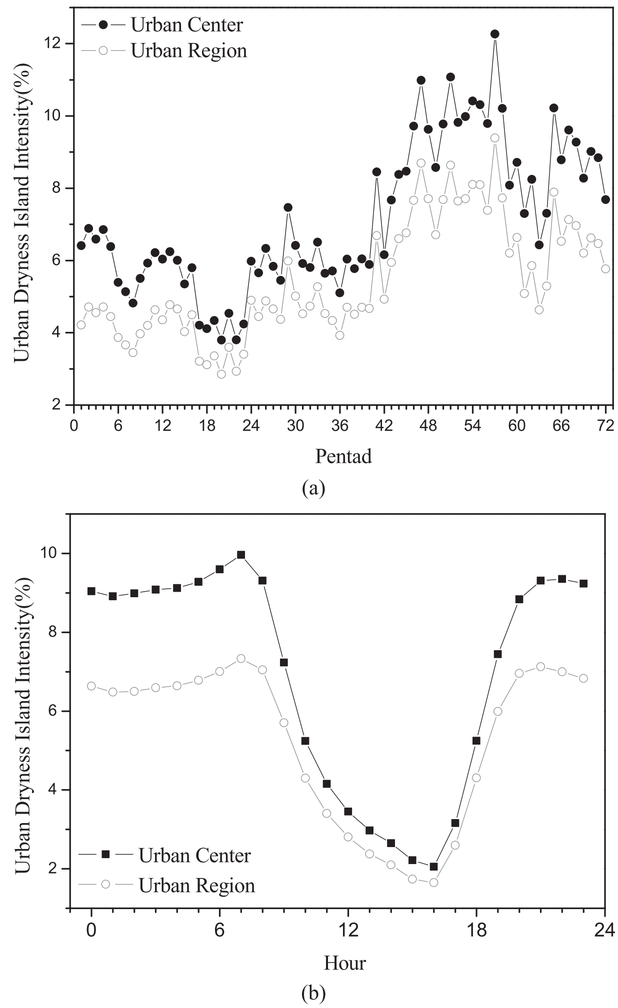

FIG. 9. (a) Pentad average UDII and (b) diurnal variation of UDII in the Beijing urban center and urban region during 2007–15.

evening. Second, the seasonal mean UDII of the different seasons varies. Table 2 and Fig. 10 show that the strongest UDII occurs in autumn and the second strongest UDII in summer, while spring sees the weakest UDII. Third, the diurnal ranges of the mean hourly UDII values in each season are also different, with the largest fluctuations in autumn and the smallest in summer.

The UDII mainly depends on the contrast of the near-surface moisture and temperature between urban and rural areas. Although the UHII values of Beijing urban areas in winter are strong, the atmospheric moisture and RH are low in both urban and rural areas, and the difference in the RH between urban areas and rural areas is small in winter and spring. The largest values of the summer and autumn hourly mean UDII appear in evening rather than in the early morning like winter and

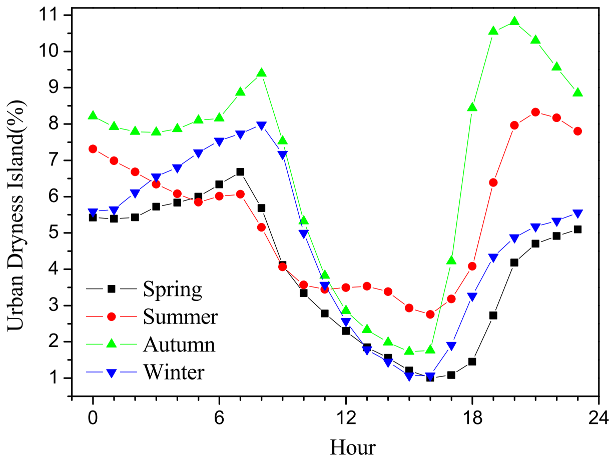

FIG. 10. Diurnal variation of seasonal mean UDII in Beijing city during 2007–15.

spring, probably because the soil and atmospheric moisture content in rural areas is higher, and the increase of the mean hourly RH values in urban areas in the evening is relatively slower than in rural areas because of the rapid rise of the UHII, resulting in an increase in the UDII until 2100 LT. After about 2100 LT, the UHII enters a plateau stage, and stronger UHI circulation is established, bringing in more humid air from rural areas to urban areas and to some extent buffering the drop of the urban RH values. This may cause a decrease in the mean hourly RH difference between urban and rural areas and a slowly downward change of the UDII.

Month–year and hour–year profiles of hourly mean UDII are shown in Figs. 11a and 11b, respectively. It is clear from Fig. 11a that any year can be divided into two parts, the first half-year (January–June) characterized by smaller UDII values and the second half-year (July–December) characterized by larger UDII values. For the first half-year, interannual variability seems also larger, with 2007–08 and 2011–12 seeing a very low monthly mean UDII value. For the second half-year, the monthly mean UDII persistently maintains a high level and interannual variability is relatively small. In autumn, a large monthly mean UDII value in every year can be clearly seen. These are consistent with the features shown in Figs. 9a and 10.

Figure 11b shows the year-to-year variations of the hourly mean UDII value in urban areas. The diurnal variation is apparent in all years. The hourly mean UDIIs steadily maintains high levels during the nighttime and lower values during the daytime in every year. However, the strength and length of the respective high- and low-value periods are not completely similar for each year. The large-value levels of UDII in 2007 and 2011 are smaller than those in other years, for example, while the lengths of low-value periods in the two years are also longer.

Figure 12 shows hour-pentad profiles of hourly mean UDII values for both UC and UR in Beijing for the time period 2007–15. Considerable differences exist between the UC and UR. In the UC, the hourly mean UDII can reach as high as 19% during the later hours of the strong UDII stage in autumn, approximately 10% larger than that in spring. A similar feature is also found for the UR, but the disparity among the seasons is smaller. Between UC and UR, the peak UDII appearance times are also slightly different. The maximum UDII value of the UC is 19.4% around 2000 of the 57th pentad (middle autumn), while that of the UR is 15.6% around 1900 of the same pentad.

Another interesting phenomenon is that the hourly mean UDII shows obviously larger values in the evening and early night in late summer and early to midautumn than those in other seasons. The largest UDII values appear at about 2000 in early to midautumn. This characteristic can also be seen in Fig. 12b, but it is less dynamic than in Fig. 12a. The hourly mean UDII values in the late night and early morning of autumn and winter display the second largest values, but the UDII magnitudes are smaller and the distribution of the high-value belts is discontinuous. The smallest UDII value is mainly centered in the afternoon hours of spring and winter, with some records around 1600 of late winter and early to midspring, which are well below 2%. Another small-value center appears in the early afternoon of late autumn. It is thus interesting to note that the largest diurnal variation in the UDII values actually occurs in midautumn (57th–58th pentad), with the early afternoon registering the smallest values of the whole yearday and the evening and early night having the largest values of the whole yearday.

TABLE 2. As in Table 1, but for UDII.

		Spring	Summer	Autumn	Winter
Mean value (%)		3.95	5.40	6.84	4.81
Daily peak	Value (%)	6.68	8.33	10.81	7.98
	Appearance time	7 h	21 h	20 h	8 h

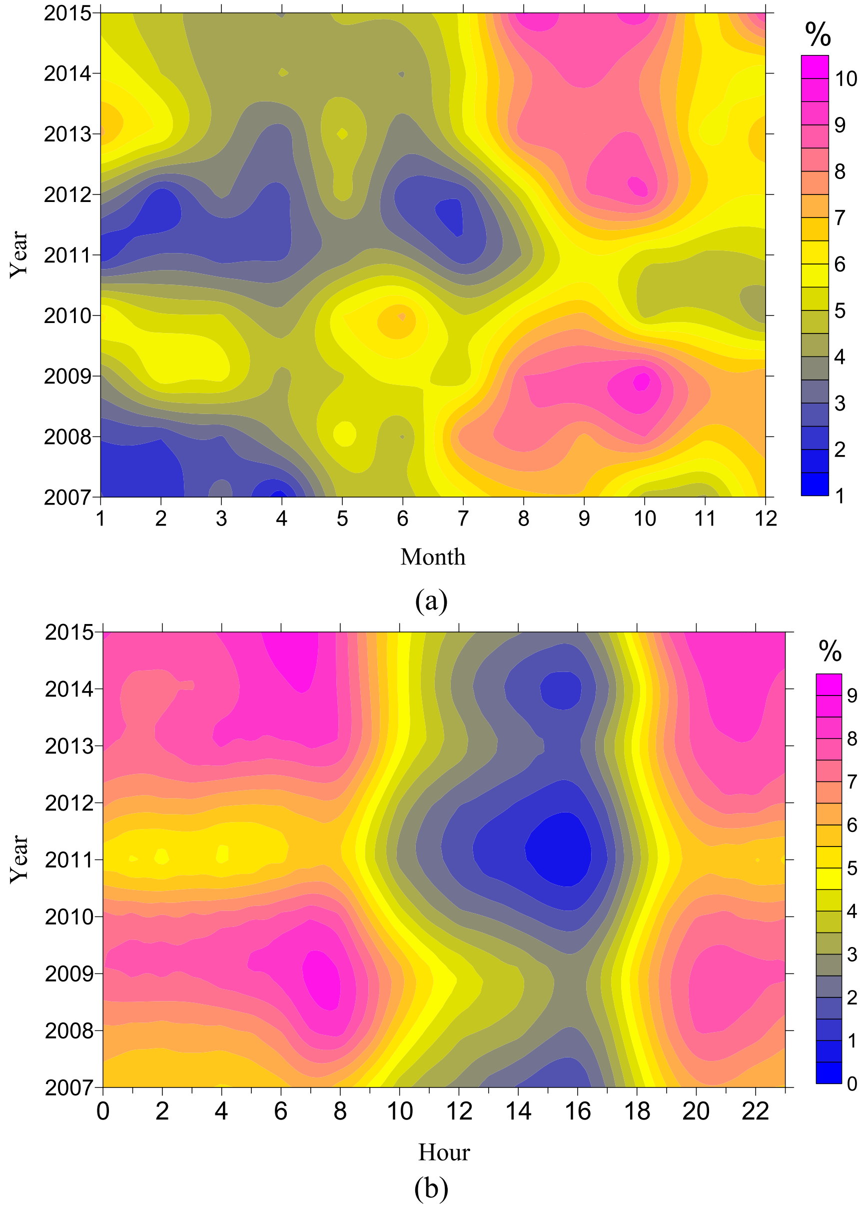

FIG. 11. (a) Month–year and (b) hour–year plots of mean UDII.

The detailed temporal structure of the UDII is obviously similar to that of the UHII in Beijing (Yang et al. 2013), and both exhibit much larger values in the evenings and nights of autumn and winter than those in the late mornings and afternoons of spring and summer. However, the strongest seasonal mean UHII occurs in winter, unlike the UDII, which occurs in autumn, and the weakest seasonal mean UHII occurs in summer, unlike the UDII, which occurs in spring. Moreover, the duration of the strong UDII stage is longer in UC than that in UR, while the minimum UDII is also smaller in the UC than that is UR (Figs. 12a,b). Both UC and UR witness a minimum of hourly mean UDII at about 2000 of the 57th pentad, but the value in the UC is slightly smaller (−0.35%) than that in the UR (−0.29%), indicating that the diurnal variation is more significant in the central urban areas than in the whole urban areas.

5. Discussion

Previous research has explored the feature of humidity by using different measuring indicators, including dewpoint temperature, vapor pressure, and relative humidity. Hage (1975) calculated urban–rural differences

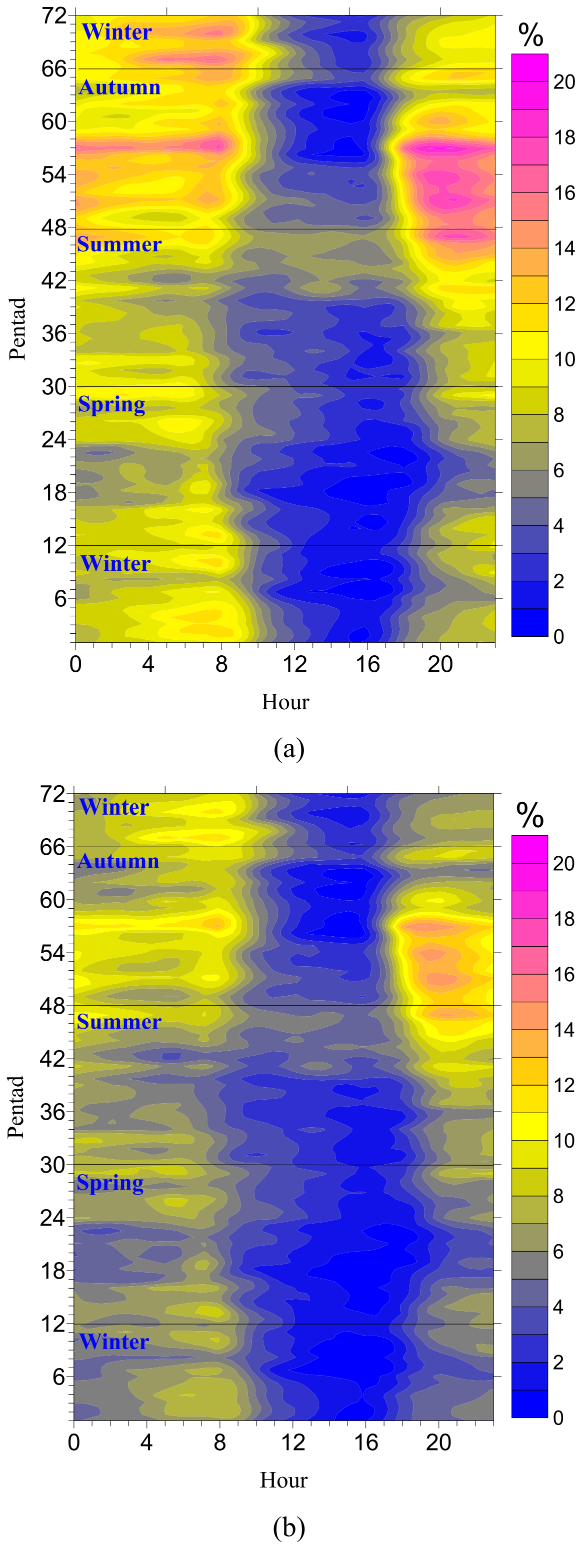

FIG. 12. Hour–pentad plots of UDII for the Beijing (a) urban center and (b) urban region.

both for absolute and relative humidity at night from airport observation in Edmonton, Alberta, Canada, and presented the similar seasonal and diurnal variation patterns of the indicators. Adebayo (1991) found that the general conditions of vapor pressure followed almost a similar trend to that of relative humidity. Previous studies indicated that although humidity indicators are various, the basic features descripted by different measuring are approximately consistent. Out of those indicators, RH is used more popularly because of its simple mathematical expression and the easiness to understand. On the whole, the general characteristics shown in this paper are generally in accordance to those reported in the previous studies (e.g., Hage 1975; Adebayo 1991; Cuadrat et al. 2015). However, a few interesting phenomena have been found in the paper probably because of the usage of a quality-controlled and densely distributed hourly dataset in the East Asian temperate megacity.

The relationship between RH and temperature is an interesting topic. To demonstrate how much of the RH variations are accounted for by temperature variations, the plots of relationship between hourly mean RH and hourly mean temperature in the central area (inside the fourth RR) have been shown in Fig. 13. It is obvious that the hourly mean RH values are higher during the nighttime with lower hourly mean temperatures (marked by blue plots), whereas the RH values are lower in the afternoon with higher temperatures (marked by green plots). This is in accordance with the result shown in Fig. 4, indicating a good negative correlation of the two variables. Therefore, diurnal variation of hourly RH almost represents a reverse trend of temperature in the central area of Beijing city. Similar conclusions are also drawn in previous research (e.g., Adebayo 1991; Fortuniak et al. 2006). This relationship is easily understandable because temperature is playing a dominant role in determining the RH in a day when the absolute moisture in the air is less variable.

Although the average diurnal variation of RH shows a consistently opposite trend with that of surface air temperature, the month–year profile of mean RH (Fig. 5) presents an obvious positive correspondence with temperature variations. This positive correlation is also remarkable in the plots of relationship between monthly mean temperature and monthly mean RH for 42 stations of urban areas in Beijing city for the period 2007–15 (Fig. 14). It is apparent that monthly mean RH has a significant positive correlation with monthly mean surface air temperature (both higher in summer and lower in winter).

Figure 15 shows the correlations between area-averaged monthly mean RH and monthly mean temperature for

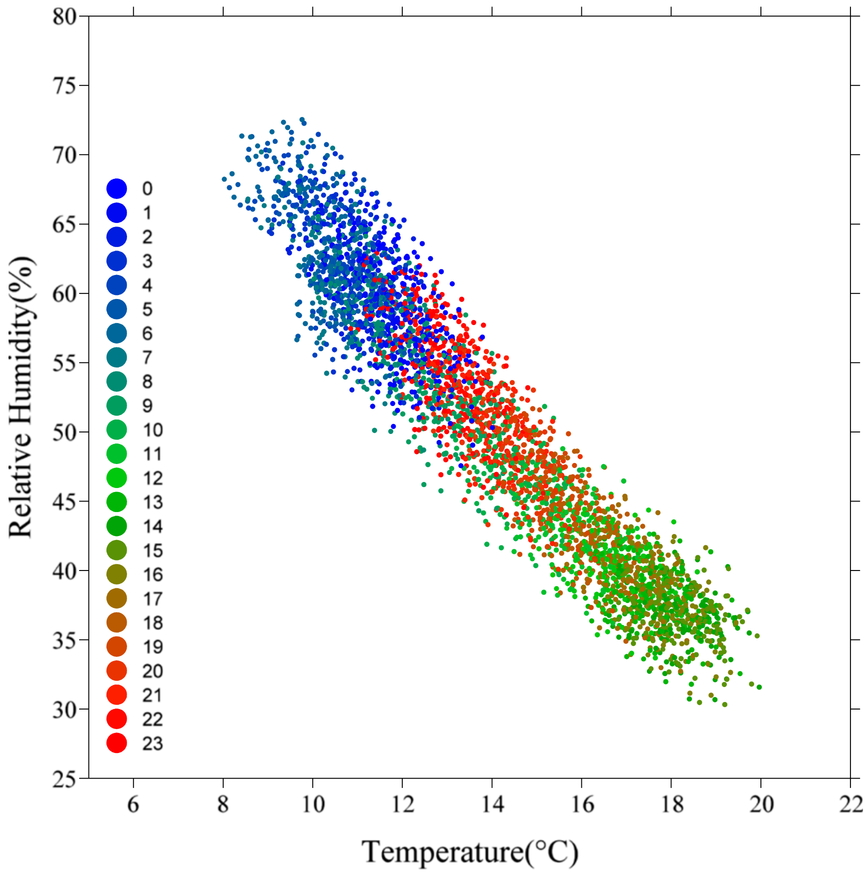

FIG. 13. The relationship between hourly mean RH (%) and hourly mean temperature (°C) per year during 2007–15 inside the Beijing city fourth RR. The different colored circles represent the hours during one day, as listed in the key.

different urban areas inside the fourth RR, between the fourth and fifth RR, and between the fifth and sixth RR. Once again, the reverse linear correlation in diurnal scale disappears when seasonal variations are concerned. Similar to Fig. 14, the positive correlations between monthly mean temperature and monthly mean RH are found for each of the urban areas (Fig. 15). It is also clear that, the more urbanized the areas are, the lower the mean monthly RHs. Moreover, different seasons show different characteristics. The area-averaged monthly RHs are very low with medium surface air temperature in three months of spring, whereas at the similar temperature range the values of RH are much higher in autumn. For the other two seasons, RHs are low with low temperature in winter and RHs are large with high temperature in summer.

The reversal of the RH–temperature relationships from diurnal to seasonal scales is also understandable, because RH is dependent on not only temperature but also moisture flux and surface evaporation. Thus, although the diurnal variation of hourly RH almost represents a reverse trend of surface air temperature, the monthly and seasonal mean RH obviously has a similar variation with surface air temperature. The relationship of RH with temperature is therefore scale dependent.

The negative correlation of hourly mean RH with hourly mean air temperature can be related to the closely linked interaction among solar irradiance, surface air temperature, and relative humidity. Air temperature increases with an increase in solar radiation intensity during the daytime, and the higher air temperature will result in a reduction of relative humidity in case of constant absolute atmospheric moisture, and at the same time will also enhance vertical mixing, which allows water vapor near the ground to reach higher altitudes, causing the RH near the ground surface to decrease until around 1500 LT, when the urban maximum surface air temperature is reached. After that, the RH near the ground increases with a decrease in surface air temperature. However, the water vapor content is still high because of the slower temperature decline due to

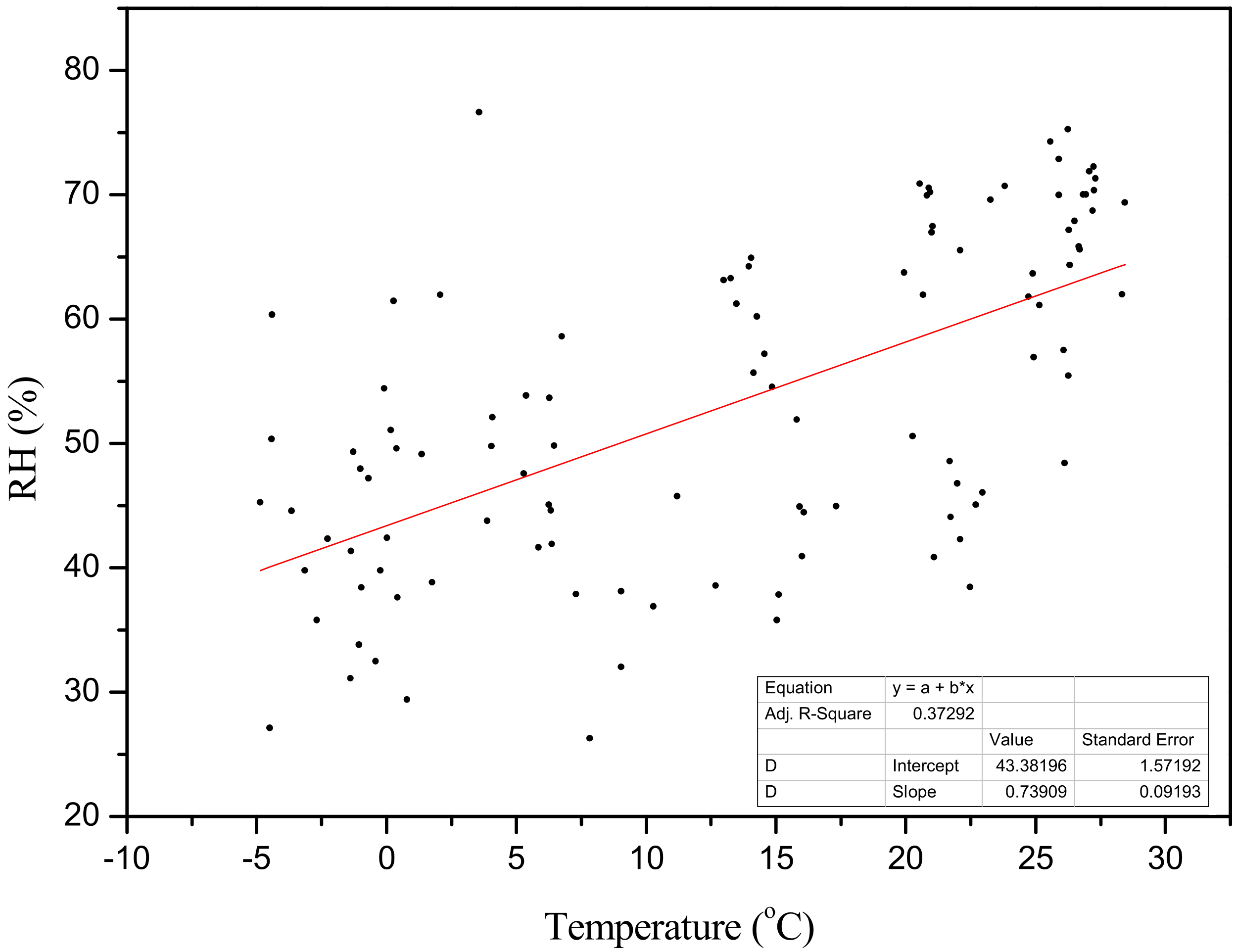

FIG. 14. The relationship between monthly mean RH (%) and monthly mean temperature (°C) for all the stations in the urban areas.

the UHI effect (Taha 1997; Dou et al. 2015) and the weakening of the vertical mixing, leading to a further increase in RH. The RH also has obvious interannual and seasonal variations as seen in Fig. 5. The larger interannual variations mainly occur in winter, however, which is probably related to more frequent invasions of strong cold and dry air masses from Mongolia and Siberia, and less stable snow cover in some years.

We have defined UDI and UDII, referring to previous works (Zhou 1994; Liu et al. 2009, 2012). An intense UDI phenomenon in Beijing city has been found in our research. Seasonally spatial distributions of UDII present evidence that UDII in autumn is most remarkable among all seasons. Adebayo (1991) found that urban influence on RH was more intense under drier conditions. Autumn in Beijing city is not the driest season, however, and the driest climate usually appears in winter and spring. This may show that the urbanization effects on seasonal mean relative humidity are different for various climate zones.

The strong UDII in the urban areas would be mainly caused by the increased impermeable land surface extents. For the latest decade, the built-up areas of Beijing city have increased 7000 ha (Qiu 2014). The expansion of impermeable land surface decreases the linkage between oil and air, which will hamper the evaporation process of soil surface (Oke 1988). Because of the large amount of impermeable land in urban areas, large amounts of rain flow through the sewage pipes instead of soil surface. In conditions of the East Asian monsoon climate, rainfall events are concentrated in summer and frequently appear as torrential rains in short periods, leading to a more rapid draining off of the surface water and a lengthening drying of the urban canopy relative to rural areas. The semiarid climate, the sparser vegetation, and the limited lakes and ponds may have also accelerated the drying process in the urban areas of the city.

The largest UDII observed in autumn may be related to the fact that, although the rainy season has ended, the

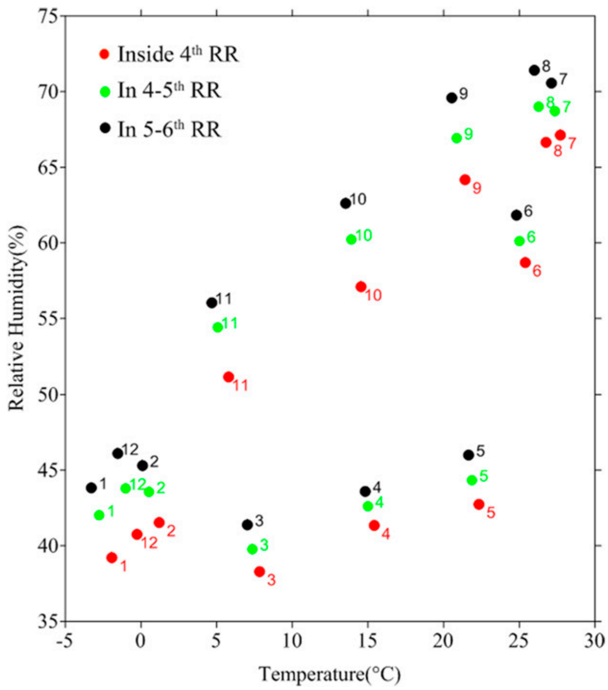

FIG. 15. The relationship between area-averaged monthly mean RH (%) and temperature (°C) during 2007–15. The circles with different colors represent different urban areas: inside the fourth RR (red), between the fourth and fifth RR (green), and between the fifth and sixth RR (black). The number marked near each dot represents different months from January to December (marked by 1–12).

soil in the rural areas still remains wet, and the difference of the relative humidity between urban and rural areas reaches its maximum. Dry seasons (winter and spring) are characterized by much less moisture in atmosphere, and the moisture difference between urban and rural areas is generally small. Cuadrat et al. (2015) showed that winds may cause greater uncertainty regarding the pattern of the UDI. In Beijing, the differences of wind speed between urban and rural areas are larger in spring and winter than in summer and autumn (Dou et al. 2015). The seasonal variation of the wind speed difference may have contributed to the average values and stability of UDI to a certain extent in spring and winter. However, the association of the UDI with wind speed needs further examination in the future.

Because of the usage of high-density hourly data, the urban center could be separated from the urban region in Beijing, and the UDII difference between urban center and urban region can be clearly exhibited (Fig. 9). The difference between urban center and urban region during nighttime is much larger than that of daytime, in particular in late summer and autumn. The difference is easily understandable, because the denser population and buildings, and the resulting stronger anthropogenic activities, are distributed in the urban center. The hourly mean UDII in both urban center and urban region has a generally larger value in the evening and early night in late summer and early to midautumn. The nocturnal UDII maximum is obviously caused by both the higher UHII and surface air temperature in the urban region and the more near-surface moisture in rural areas during the evening and nighttime. However, more research on the interactions of surface air temperature, atmospheric water vapor, soil moisture, horizontal advection, vertical turbulent flux, and radiative flux is still needed in order to better understand the physical processes important in forming the spatial and temporal characteristics of the UDII in Beijing city.

The implications of the significant UDII for planning and management of urban development and environmental protection in Beijing city are not so clear. The urban areas are becoming drier with the urbanization, but this does not mean that the total and intense precipitation has been decreasing. Actually, total and short-duration intense precipitation during summertime increased relative to the rural areas (Sun and Shu 2007; Yang et al. 2017). What have been observed are the simultaneous reduction of atmospheric relative humidity and the rise of warm-season precipitation, accompanied by a drying air and an increasing risk of logging and flooding over the urban areas. The drying urban boundary layer atmosphere will undoubtedly increase the potential and actual evaporation and transpiration at the surface, leading to a higher water demand for irrigation of urban ecosystems (Yang and Wang 2015), and it may also increase the risk of fire disasters especially in autumn. However, the drying air during the hot and wet seasons (summer) would help ease thermal stress and the negative impact of heat waves in the urban areas. Actually, study has found that, although the temperature in summer over Beijing has increased for the latest years, human comfort has not decreased in Beijing urban areas because of the existence of UDI (Wang and Gong 2010). In this sense, the large UDI as reported here also has a positive impact on some aspects. The other potential impacts of the UDI effect on urban ecosystems, environment, and human health could be further investigated in future.

6. Conclusions

This paper examined the climatological characteristics of the RH and UDI phenomena in Beijing urban areas by applying a quality-controlled hourly dataset obtained from a high-density AWS network. The following conclusions are drawn from the study:

1) Small annual mean and seasonal mean RH values occur mostly in central urban areas or nearby zones. The largest monthly mean RH values occur in July, August, and September.
2) Hourly mean RH values reached a minimum of 37.5% at 1500 LT and a maximum of 67.2% at 0600 LT during the day. For all seasons, the hourly mean RH peaks in early morning, stays low from 1200 to 1600 LT, and increases from 0400 to 0700 LT. The decreasing rate in the morning is much larger than the increasing rate in afternoons and early evenings.
3) The annual mean UDII reaches more than 8% in central urban areas, and the autumn mean UDII values can be as large as 12%–15% inside the fourth RR. The smallest UDII values, approaching zero, appear in winter and spring months in outer urban areas or suburban zones.
4) The diurnal UDII variations are characterized by a steadily strong UDII stage from 2000 to 0800 LT and a minimum at 1500 or 1600 LT. The rapid shifts from high to low and from low to high values occur during the periods 0800–1600 and 1600–2000 LT, respectively. The occurrence time of the peaks varies among the different seasons, and they appear at 0700, 2100, 2000, and 0800 LT for spring, summer, autumn and winter, respectively.
5) Large UDII values appear in the evenings and early nights of late summer and early to midautumn. The hourly mean UDII in central urban areas can reach more than 15% during the strong UDII hours in autumn, with the maximum UDII value being 19.4% occurring around 2000 of the 57th pentad (midautumn). Small UDII values occur mainly in the afternoon hours of spring, winter, and late autumn.

Acknowledgments. This study is financially supported by the China Natural Science Foundation (CNSF) (Funds 41375069, 41575003, and 41675092) and the Ministry of Science and Technology of China (Fund GYHY201206012).

REFERENCES

Ackerman, B., 1971: Moisture content of city and country air. Preprints, *Conf. on Air Pollution Meteorology*, Raleigh, NC, Amer. Meteor. Soc., 154–158.

——, 1987: Climatology of Chicago area urban–rural differences in humidity. *J. Climate Appl. Meteor.*, **26**, 427–430, doi:10.1175/1520-0450(1987)026<0427:COCAUR>2.0.CO;2.

Adebayo, Y. R., 1991: Day-time effects of urbanization on relative humidity and vapour pressure in a tropical city. *Theor. Appl. Climatol.*, **43**, 17–30, doi:10.1007/BF00865039.

Ayoade, J. O., 1983: *Introduction to Climatology for the Tropics.* Wiley, 258 pp.

Chandler, T. J., 1967: Absolute and relative humidities in towns. *Bull. Amer. Meteor. Soc.*, **48**, 394–399.

China Meteorological Administration, 2003: *Specification of Ground Meteorological Observation*, China Meteorological Press.

Cuadrat, J. M., S. Vicente-Serrano, and M. A. Saz, 2015: Influence of different factors on relative air humidity in Zaragoza, Spain. *Front. Earth Sci.*, **3**, doi:10.3389/feart.2015.00010.

Dou, J. J., Y. C. Wang, and S. G. Miao, 2015: Observed spatial characteristics of Beijing urban climate impacts on summer thunderstorms. *J. Appl. Meteor. Climatol.*, **54**, 94–104, doi:10.1175/JAMC-D-13-0355.1.

Fortuniak, K., K. Klysik, and J. Wibig, 2006: Urban–rural contrasts of meteorological parameters in Łódź. *Theor. Appl. Climatol.*, **84**, 91–101, doi:10.1007/s00704-005-0147-y.

Hage, K. D., 1975: Urban–rural humidity difference. *J. Appl. Meteor.*, **14**, 1277–1283, doi:10.1175/1520-0450(1975)014<1277:URHD>2.0.CO;2.

Han, J. Y., and J. J. Baik, 2008: A theoretical and numerical study of urban heat island-induced circulation and convection. *J. Atmos. Sci.*, **65**, 1859–1877, doi:10.1175/2007JAS2326.1.

Hilberg, S. D., 1978: Diurnal temperature and moisture cycles. *Summary of METROMEX*, Vol. 2, *Causes of Precipitation Anomalies*, Illinois State Water Survey Bull. 63, Champaign, IL, 25–42. [Available online at http://www.isws.illinois.edu/pubdoc/B/ISWSB-63.pdf.]

Jáuregui, E., 1973: The urban climate of Mexico City. *Erdkunde*, **27**, 298–307, doi:10.3112/erdkunde.1973.04.06.

Karl, T. R., H. F. Diaz, and G. Kukla, 1988: Urbanization: Its detection and effect in the United States climate record. *J. Climate*, **1**, 1099–1123, doi:10.1175/1520-0442(1988)001<1099:UIDAEI>2.0.CO;2.

Kothawale, D., N. Deshpande, and R. Kolli, 2016: Long term temperature trends at major, medium, small cities and hill stations in India during the period 1901-2013. *Amer. J. Climate Change*, **5**, 383–398, doi:10.4236/ajcc.2016.53029.

Kratzer, P. A., 1956: *The Climate of Cities.* Friedrich Vieweg Sohn, 184 pp.

Landsberg, H. E., 1981: *The Urban Climate.* Academic Press, 275 pp.

Lee, D. O., 1991: Urban–rural humidity difference in London. *Int. J. Climatol.*, **11**, 577–582, doi:10.1002/joc.3370110509.

Li, J., R. Swinbank, R. Grotjahn, and H. Volkert, 2016: *Dynamics and Predictability of Large-Scale, High-Impact Weather and Climate Events*. Special Publications of the International Union of Geodesy and Geophysics, Cambridge University Press, 370 pp.

Lin, Z. H., X. G. Mo, H. X. Li, and H. B. Li, 2002: Comparison of three spatial interpolation methods for climate variables in China. *Acta Geogr. Sin.*, **57**, 47–56.

Liu, M. C., X. L. Yang, Y. C. Yin, and J. G. Hu, 2012: Climate characteristics and forecast of relative humidity in Wuwei City. *Arid Zone Res.*, **29**, 655–659.

Liu, W. D., H. L. You, and J. X. Dou, 2009: Urban–rural humidity and temperature differences in the Beijing area. *Theor. Appl. Climatol.*, **96**, 201–207, doi:10.1007/s00704-008-0024-6.

Liu, X. D., Z. Y. Yin, X. Y. Zhang, and X. C. Yang, 2004: Analyses of the spring dust storm frequency of northern China in relation to antecedent and concurrent wind, precipitation, vegetation, and soil moisture conditions. *J. Geophys. Res.*, **109**, D16210, doi:10.1029/2004JD004615.

Moriwaki, R., K. Watanabe, and K. Morimoto, 2013: Urban dry island phenomenon and its impact on cloud base level. *J. JSCE*, **1**, 521–529, doi:10.2208/journalofjsce.1.1_521.

Morris, C. J. G., I. Simmonds, and N. Plummer, 2001: Quantification of the influences of wind and cloud on the nocturnal urban heat island of a large city. *J. Appl. Meteor.*, **40**, 169–182, doi:10.1175/1520-0450(2001)040<0169:QOTIOW>2.0.CO;2.

Oke, T. R., 1982: The energetic basis of the urban heat island. *Quart. J. Roy. Meteor. Soc.*, **108**, 1–24, doi:10.1002/qj.49710845502.

——, 1988: The urban energy balance. *Prog. Phys. Geogr.*, **12**, 471–508, doi:10.1177/030913338801200401.

Padmanabhamurty, B., and H. D. Bahl, 1982: Some physical features of heat and humidity islands at Delhi. *Mausam*, **33**, 211–216.

Qiu, H. L., 2014: Study on urban heat island effect and cooling effect of green land in Beijing. Doctoral thesis, Beijing Forestry University, 107 pp.

Ren, G. Y., and Y. Q. Zhou, 2014: Urbanization effects on trends of extreme temperature indices of national stations over mainland China, 1961–2008. *J. Climate*, **27**, 2340–2360, doi:10.1175/JCLI-D-13-00393.1.

——, Z. Y. Chu, Z. H. Chen, and Y. Y. Ren, 2007: Implications of temporal change in urban heat island intensity observed at Beijing and Wuhan stations. *Geophys. Res. Lett.*, **34**, L05711, doi:10.1029/2006GL027927.

Ren, Y. Y., and G. Y. Ren, 2011: A remote-sensing method of selecting reference stations for evaluating urbanization effect on surface air temperature trends. *J. Climate*, **24**, 3179–3189, doi:10.1175/2010JCLI3658.1.

Robaa, S. M., 2013: Some aspects of the urban climates of greater Cairo region, Egypt. *Int. J. Climatol.*, **33**, 3206–3216, doi:10.1002/joc.3661.

Song, Y., Y. Liu, and Y. Ding, 2012: A study of surface humidity changes in China during the recent 50 years. *Acta Meteor. Sin.*, **26**, 541–553, doi:10.1007/s13351-012-0501-9.

Sun, J. S., and W. J. Shu, 2007: Impact of UHI effect on winter and summer precipitation in Beijing City. *Atmos. Sci.*, **31**, 311–320.

Taha, H., 1997: Urban climates and heat islands: Albedo, evapotranspiration, and anthropogenic heat. *Energy Build.*, **25**, 99–103, doi:10.1016/S0378-7788(96)00999-1.

Unkašević, M., O. Jovanović, and T. Popović, 2001: Urban-suburban/rural vapor pressure and relative humidity differences at fixed hours over the area of Belgrade city. *Theor. Appl. Climatol.*, **68**, 67–73, doi:10.1007/s007040170054.

Wang, X. L., X. R. Li, and Z. K. Feng, 2010: Research on urban extension based on Shannon entropy. *China Popul. Res. Environ.*, **20**, 88–92.

Wang, X. Q., and Y. B. Gong, 2010: Impact of urban dryness island on summer heat wave severity in Beijing. *Chin. Sci. Bull.*, **11**, 1043–1047.

Wang, Z. H., 2014: A new perspective of urban–rural differences: The impact of soil water advection. *Urban Climate*, **10**, 19–34, doi:10.1016/j.uclim.2014.08.004.

Yang, J. H., and Z. H. Wang, 2015: Optimizing urban irrigation schemes for the trade-off between energy and water consumption. *Energy Build.*, **107**, 335–344, doi:10.1016/j.enbuild.2015.08.045.

Yang, P., W. D. Liu, J. Q. Zhong, and J. Yang, 2011: Evaluating the quality of temperature measured at Automatic Weather Stations in Beijing. *J. Appl. Meteor. Sci.*, **22**, 706–715.

——, G. Y. Ren, and W. D. Liu, 2013: Spatial and temporal characteristics of Beijing urban heat island intensity. *J. Appl. Meteor. Climatol.*, **52**, 1803–1816, doi:10.1175/JAMC-D-12-0125.1.

——, Z. N. Xiao, and M. S. Ye, 2016: Cooling effect of urban parks and their relationship with urban heat island. *Atmos. Ocean. Sci. Lett.*, **9**, 298–305, doi:10.1080/16742834.2016.1191316.

——, ——, and W. J. Shi, 2017: Fine-scale characteristics of rainfall in Beijing urban area based on a high-density AWS dataset (in Chinese). *Chin. J. Atmos. Sci.*, **41**, 475–489, doi:10.3878/j.issn.1006-9895.1606.16134.

Zhang, G. H., Z. C. Li, Y. Song, Y. L. Wu, and X. L. Wang, 2011: Spatial patterns of change trend in rainfall of China and the rope of East Asia summer monsoon. *Arid Land Geogr.*, **34**, 34–42.

Zhou, S. Z., 1994: Discussion of the urban–rural differences in atmospheric humidity of Shanghai area. *Trans. Oceanol. Limnol.*, **2**, 13–25.